

The large-scale *rms* bulk velocity estimated from QSOs' Ly α forests

Hu Zhan and Li-Zhi Fang

Department of Physics, University of Arizona, Tucson, AZ 85721

ABSTRACT

We propose a method for estimating the large-scale *rms* bulk velocity of the cosmic mass field from the transmitted fluxes of Ly α forests. It is based on two linear relationships on large scales: 1) the relation between the fluctuations of the transmission and the underlying density field, and 2) the relation between the density fluctuations and the peculiar velocity field. We show that, with a multi-scale decomposition, the two relations can be effectively employed for predicting the *rms* bulk velocity. Since QSO's Ly α forest is due to the absorptions of diffusely distributed and photoionized IGM, this method provides an independent estimate of the *rms* bulk velocity at high redshifts, on large scales, and free from the bias of galaxies. Using the transmitted flux of 60 moderate-resolution QSO spectra, the *rms* bulk velocity is found to be 230 ± 50 km s $^{-1}$ around redshift $z = 2.25$ on scale 23 h $^{-1}$ Mpc, and down to 110 ± 45 km s $^{-1}$ around $z = 3.25$ on scale 92 h $^{-1}$ Mpc for an LCDM universe ($\Omega = 0.3$ and $\Lambda = 0.7$). The results are basically consistent with the linear evolution theory.

Subject headings: cosmology: theory - large-scale structure of universe

1. Introduction

The transmitted fluxes of high redshift QSOs' Ly α absorption spectra have been successfully applied to many aspects of cosmic large-scale structure study, such as the discrimination among dark matter models (Bi, Ge & Fang 1995; Bi & Davidsen 1997), recovery of the initial linear mass power spectrum and estimation of cosmological parameters (Croft et al. 1998 & 1999; Hui 1999; Nusser & Haehnelt 1999; McDonald & Miralda-Escudé 1999; Feng & Fang 2000; McDonald et al 2000), and finding the applicable range of the hierarchical clustering model (Feng, Pando & Fang 2001; Zhan, Jamkhedkar & Fang 2001). These studies show that Ly α forests provide an important complement to structure formation studies based on galaxy samples.

In this paper we extend the application of Ly α forests to the cosmic velocity field. In terms of cosmological parameter determination, the *rms* bulk velocity is an important statistic, as it is related to an integrated power spectrum over the scales beyond the directly detectable range of the power spectrum with current galaxy surveys. On such scales, the cosmic clustering remains in the linear regime, and, therefore, would be useful to set a constraint on cosmological parameters, and on the relation between the galaxy distribution and the underlying mass field.

Many efforts have been made on measuring and estimating cosmic bulk velocity with galaxy samples. An important result is that the velocity field calculated from spatial distribution of galaxies is found to be basically consistent with the peculiar velocities measured based on the Tully-Fisher or fundamental plane relations (e.g. Dekel et al 1999; Branchini et al 1999). This indicates that the bulk velocity of galaxies on large scale is of gravitational origin. That is, the cosmic velocity field $\mathbf{v}(\mathbf{x})$ on large scales is related to the cosmic mass density field $\delta(\mathbf{x})$ via the following linear relation or its variants

$$\delta(\mathbf{x}) = -\frac{1}{H_0 f} \nabla \cdot \mathbf{v}(\mathbf{x}), \quad (1)$$

where $f \simeq \Omega^{0.6}$ for the local universe. We define $\mathbf{x} = (x, y, r)$, where x and y are the coordinates on the celestial sphere, and r is the radial or redshift direction.

A problem with galaxy samples, however, arises from the likely bias of the distributions of galaxies relative to the underlying mass distribution in the universe. The simplest bias model assumes that the number density fluctuations of galaxies, $\delta_g(\mathbf{x})$, is related to the underlying mass density field by $\delta_g(\mathbf{x}) = b\delta(\mathbf{x})$, where b is the bias parameter. More sophisticated models assume that the relation between $\delta_g(\mathbf{x})$ and $\delta(\mathbf{x})$ might be stochastic, non-local, and non-linear. Furthermore, the peculiar velocities of galaxies may also be biased from the cosmic velocity field. These effects will cause uncertainty in deriving the cosmic velocity field from galaxy samples. It is therefore important to develop a method of estimating the cosmic velocity field free from galaxy bias.

Here we calculate, based on Eq. (1), the large-scale *rms* bulk velocities from samples of the transmitted flux F of QSO's Ly α absorption spectrum. The QSO Ly α forest is very well modeled by absorption from diffusely distributed and photoionized IGM, which in turn is believed to be distributed proportionally to the density of the underlying mass field $\rho(\mathbf{x})$ on scales larger than the Jeans length of the IGM (for a review, see Rauch 1998). The transmitted flux of QSO's Ly α forest is thus likely to be less biased as a tracer of the underlying mass and velocity field, providing an independent estimate of the *rms* bulk velocity, separate from that defined by galaxies.

To do so, we need to develop methods for: 1) Obtaining mass fluctuation data $\delta(\mathbf{x})$ from

Ly α flux F in QSO spectra, in the linear or quasi-linear regimes. 2) Properly calculating the bulk velocity from mass fluctuations. These two methods are discussed, respectively, in §2 and §3. The results of our investigation of the *rms* bulk velocity on large scales at high redshifts are presented in §4.

2. Probability Distribution Function of Ly α Transmission

2.1. Transmission–density relation

For a QSO with coordinate (x_i, y_i) on the celestial sphere, the observed flux of Ly α absorptions is equal to $F_c e^{-\tau(z)}$, with F_c being the continuum, and $\tau(z)$ the optical depth. The data to be used have been normalized, and therefore the transmission $F(z) = e^{-\tau(z)}$.

For a diffusely distributed HI cloud in photoionization equilibrium, we have (e.g. Bi 1993; Fang et al. 1993)

$$\tau(z) = A(z) \int dr [1 + \delta(x_i, y_i, r)]^a V[w(z) - r - v_r(x_i, y_i, r), b] \quad (2)$$

where $w(z)$ is the redshift space coordinate, r is the radial comoving coordinate, V is the normalized Voigt profile that is approximately Gaussian, $V \simeq 1/(\sqrt{\pi}b) \times \exp\{-[w(z) - r - v_r(x_i, y_i, r)]^2/b^2\}$, $v_r(x_i, y_i, r)$ is the radial component of peculiar velocity, b is the Doppler broadening on the order of several tens km s $^{-1}$, and $\delta(x_i, y_i, r) = [\rho(x_i, y_i, z) - \bar{\rho}]/\bar{\rho}$ is the dark matter density contrast smoothed on the scale of the IGM Jeans length (e.g. Bi & Davidsen 1997; Nusser & Haehnelt 1999). The parameter $A(z)$, which depends on the cosmic baryonic density, the photoionization rate of HI, and the mean temperature of IGM, is referred to the mean transmission over a redshift range as $\langle F(z) \rangle = \langle e^{-\tau(z)} \rangle = e^{-A(z)}$. The parameter a depends on reionization, and is in the range of 1.5 to 1.9 (Hui & Gnedin 1997).

There are two problems in drawing information of linear or quasi-linear density fluctuations δ from the transmitted flux F . First, the relation between F and δ is non-linear. This is especially true for a saturated absorption line, i.e. $F \simeq 0$ corresponds to the non-linear regime of δ . Second, the peculiar velocity v_r , which is what we are trying to detect, already enters in Eq.(2). These two problems can be avoided by considering the smoothed F and δ on large scales. If the smoothing scales are much larger than the Doppler factor b and the positional uncertainty caused by the peculiar velocity $v(x)$, the Voigt function V can be approximated as a Dirac delta function $\delta^D(r - w(z))$. In this case, Eq.(2) yields

$$F(z) \simeq \exp\{-A(z)[1 + \delta(x_i, y_i, z)]^a\}. \quad (3)$$

For simplicity, in Eq.(3) and hereafter we still use the notations $F(z)$ and $\delta(z)$ for the smoothed transmission and density perturbations. Thus, for the linear or quasi-linear regime, i.e., $|\delta F(z)| = |\delta(x_i, y_i, z)|/\langle F(z) \rangle < 1$ and $|\delta(x_i, y_i, z)| < 1$, Eq.(3) gives

$$\delta(x_i, y_i, z) \simeq -\frac{1}{aA(z)}\delta F(z), \quad (4)$$

where (x_i, y_i) is to remind that it is for the i -th QSO.

Eq.(4) shows that the fluctuations of the Ly α transmission flux $\delta F(z)$ trace the underlying density perturbation $\delta(x_i, y_i, z)$ point-by-point. The factor $aA(z)$ plays the role of a bias parameter between the Ly α flux fluctuations and the mass density perturbations. $aA(z)$ is of order of 1, as $a \simeq 1.5 - 1.9$ and $A(z) \simeq 0.75 - 0.9$. Eq.(3) has been used in the recovery of the initial linear power spectrum of the underlying mass field by the observed Ly α transmission (e.g. Croft et al. 1998). It should be reminded that Eq.(4) holds only if 1) the variance of δF is less than 1, or the variance of F is less than $\langle F(z) \rangle$; and 2) the positional uncertainty caused by the peculiar velocity is much smaller than the scales considered. We will check the validity of these conditions in the analysis below.

2.2. Transmission–density relation in DWT representation

To do the smoothing of the transmitted fluxes, we apply the algorithm of multiscale-decomposition based on the discrete wavelet transform (DWT) (Daubechies 1992; Fang & Thews 1998). Because the bases of the DWT analysis are orthogonal, complete and localized, it is easy for the calculation to use Eq.(1) (next section). In our calculation, we use the Daubechies 4 (D4) wavelets.

Let us consider a sample $\delta F(z)$ that spans a redshift space $L = z_2 - z_1$, and the spectrum is binned into 2^J pixels with J being an integer. With the DWT analysis, the smoothed $\delta F(z)$ on the scale $L/2^j$ is given by

$$\delta F_j(z) = \sum_{l=0}^{2^j-1} \epsilon_{jl}^F \phi_{jl}(z), \quad (5)$$

where $\phi_{jl}(z)$ s are the DWT scaling functions for mode (jl) . The label j is for spatial scale $L/2^j$, and l is for the position in redshift space around $z_1 + lL/2^j$. The scaling function plays the role of a window function. The scaling function coefficient (SFC) ϵ_{jl}^F is given by

$$\epsilon_{jl}^F(x_i, y_i) = \int \delta F(z) \phi_{jl}(z) dz, \quad (6)$$

where (x_i, y_i) is to show that the flux fluctuation $\delta F(z)$ in Eq.(6) is for the i -th QSO. The SFC ϵ_{jl}^F is proportional to the mean flux over a bin size $L/2^j$ around the position l . Thus, with the DWT decomposition, Eq.(4) becomes

$$\epsilon_{jl}^m(x_i, y_i) = -\frac{1}{aA(z)}\epsilon_{jl}^F(x_i, y_i), \quad (7)$$

where the SFC of the mass field is given by

$$\epsilon_{jl}^m(x_i, y_i) = \int \delta(x_i, y_i, z)\phi_{jl}(z)dz. \quad (8)$$

Therefore, Eq.(7) is the DWT representation of Eq.(4). The SFCs ϵ_{jl}^F and ϵ_{jl}^m actually are, respectively, the fluctuations $\delta F(z)$ and $\delta(z)$ in DWT representation. Eq.(7) has been used in the DWT recovery of the initial linear power spectrum of the underlying mass field by the observed Ly α transmission flux (Feng & Fang 2000).

2.3. PDF of Ly α Transmission

The samples of transmitted fluxes $F(z)$ used in our study comprise of 60 QSOs' spectra selected from Bechtold (1994), Dobrzański & Bechtold (1996), Scott, Bechtold & Dobrzański (2000), and Scott et al. (2000). The selection ensures that each spectrum in the calculation below is comparable to at least twice the length of the largest scale ($92 \text{ h}^{-1}\text{Mpc}$) interested. The emission redshift of the QSOs covers the range from 1.9 to 4.12. Each spectrum is averaged in bins of size $\sim 1.2\text{\AA}$, such that there are 1024 ‘pixels’ per unit redshift, which converts to a resolution of $c/1024 \simeq 293 \text{ km s}^{-1}$.

Using Eq.(6), we compute the SFCs ϵ_{jl}^F of flux fluctuations $\delta F(z)$ for each QSO. We use the so-called off-counting method to treat the spectra (Jamkhedkar, Bi & Fang 2001), i.e. the SFC ϵ_{jl}^F of modes (j, l) is not counted in the calculation if the data at that mode are contaminated by metal line, bad, or low S/N pixels. An advantage of the DWT off-counting method is that the statistical results on large scales are not sensitive to the bad pieces on small scales.

We treat all the data as ensembles of various modes (j, l) . That is, for a given mode (j, l) , the ensemble consists of all SFCs $\epsilon_{jl}^F(x_i, y_i)$ of the QSOs that have flux observed around $\lambda = (1 + z_1 + lL/2^j)\lambda_\alpha$, where $\lambda_\alpha \simeq 1216\text{\AA}$. Thus, we can calculate the ensemble average of SFCs of each mode (j, l) by

$$\bar{\epsilon}_{jl}^F = \frac{1}{N} \sum_{i=1}^N \epsilon_{jl}^F(x_i, y_i). \quad (9)$$

where N is the number of the SFCs in the ensemble.

Since modes (j, l) are localized in redshift space, we can also construct ensembles of the SFCs in different redshift ranges. For a given redshift range $z \pm (\Delta z/2)$, the ensemble consists of all $\epsilon_{jl}^F(x_i, y_i)$ of which the label l corresponds to position in the range $z \pm (\Delta z/2)$. In the following calculations, we use three redshift ensembles. They are $z=2.25$, 2.75 , and 3.25 with $\Delta z = 0.50$.

The probability distribution functions (PDFs) of the SFCs ϵ_{jl}^F are calculated in the three redshift ranges. The result for $z = 2.75$ is plotted in Figure 1. The scale j corresponds to redshift distance $\delta z = \Delta z/2^j = 2^{-j-1}$. In Fig. 1, the physical scale of j is calculated from the redshift distance δz at $z = 2.75$, for a LCDM model ($\Omega = 0.3$ and $\Lambda = 0.7$). For instance, the scale $92 \text{ h}^{-1} \text{ Mpc}$ corresponds to $\delta z = 0.125$, or in wavelength $\Delta\lambda \simeq 152 \text{ \AA}$.

In Figure 1, the panel on the smallest scale, i.e. $72 \text{ h}^{-1}\text{kpc}$, is the PDF of the binned distribution $F(z)$ without the SFC smoothing, and therefore, it actually is the PDF of QSO Ly α transmission, which has been done by many others (e.g. McDonald et al. 2000). Rather, Figure 1 shows the scale dependence of the PDFs. When the smoothing scale is small (large j), the PDF is significantly non-Gaussian, while it is essentially Gaussian on large scales. The K-S test shows that the PDFs are Gaussian on scales larger than $12 \text{ h}^{-1} \text{ Mpc}$, and non-Gaussian on scales less than $\sim 12 \text{ h}^{-1} \text{ Mpc}$. This is consistent with the authors' previous work (Zhan, Jamkhedkar, & Fang 2001). Moreover, the variance of $2^{(j-9)/2}\epsilon_{jl}^F$, or equivalently the variance of $\delta F_j(z)$, is less than 1. Thus, it is reasonable to calculate the density perturbations of the underlying mass field by Eqs.(4) or (7).

All the above-mentioned properties are typical. That is, in other redshift ranges, the behavior of the ϵ_{jl}^F PDFs is similar to Figure 1 with a slight evolution in the redshift range considered. Thus, on scales larger than $12 \text{ h}^{-1} \text{ Mpc}$, one can calculate the SFCs of the mass field with Eq.(7). In these cases, Eq.(7) also insures that the variance of the density fluctuations δ is less than 1, and therefore, the corresponding evolution of the mass field is still in the linear or quasi-linear regime.

3. Ly α forest estimator for *rms* bulk velocity

3.1. Density-velocity relation in DWT representation

By definition, a 1-D radial density perturbation $\delta(r)$ is given by the projection of the 3-D density perturbation $\delta(x, y, r)$ into 1-D, i.e.

$$\delta(r) = \frac{1}{L_x L_y} \int_{L_x} \int_{L_y} \delta(x, y, r) dx dy = \frac{1}{L_x L_y \bar{\rho}} \left[\int_{L_x} \int_{L_y} \rho(x, y, r) dx dy - \bar{\rho} \right], \quad (10)$$

where $L_x \times L_y$ is the area of the coverage of samples on the celestial sphere. Both L_x and L_y are larger than the scale considered in the radial (or redshift) direction. Since velocity field $\mathbf{v}(\mathbf{x})$ is statistically homogeneous, we have $(1/L_x L_y) \int_{L_y} \int_{L_x} (\partial v_x(x, y, r)/\partial x) dx dy = (1/L_y) \int_{L_y} [v_x(x_2, y, r) - v_x(x_1, y, r)]/L_x dy \simeq 0$. Similarly, $(1/L_x L_y) \int_{L_x} \int_{L_y} (\partial v_y/\partial y) dy dx \simeq 0$. Thus, subjecting Eq.(1) to the operation $(1/L_x L_y) \int_{L_x} \int_{L_y} ... dx dy$, we have a 1-D equation

$$\delta(r) = -\frac{1}{H_0 f} \frac{d}{dr} v(r), \quad (11)$$

where $v(r)$ is a 1-D velocity defined by

$$v(r) = \frac{1}{L_x L_y} \int_{L_x} \int_{L_y} v_r(x, y, r) dx dy \quad (12)$$

In redshift space, Eq.(11) is

$$\delta(z) = -\frac{1+z}{H f D} \frac{d}{dz} v(z), \quad (13)$$

where $(1+z)$ comes from the expansion of the universe, v is the radial component of the velocity field, and $D = dr/dz$. For an LCDM model with $\Omega + \Lambda = 1$, we have $D = c[H_0 E(z)]^{-1}$, $H = H_0 E(z)$, $E(z) = [\Omega(1+z)^3 + \Lambda]^{1/2}$ (Peebles 1993), and $f \equiv f(z) \approx [\Omega(1+z)^3 E(z)^{-2}]^{0.6}$ (Lahav et al. 1991).

The operator d/dz is almost diagonal in wavelet representation (Farge et al. 1996), and therefore, subjecting Eq.(13) to a DWT with scaling function $\phi_{jl}(z)$, we have

$$\epsilon_{jl}^m \simeq -\frac{1+z}{H f D} \sum_{l'=0}^{2^j-1} \epsilon_{jl'}^v \int \phi_{jl}(z) \frac{d}{dz} \phi_{jl'}(z) dz \quad (14)$$

where ϵ_{jl}^v is the SFC of the velocity field, given by $\epsilon_{jl}^v = \int v(z) \phi_{jl}(z) dz$. The SFC ϵ_{jl}^v is proportional to the bulk velocity v_j on the spatial range given by the window function ϕ_{jl} , i.e.

$$v_j = \frac{\int v(z) \phi_{jl}(z) dz}{\int \phi_{jl}(z) dz} = \sqrt{\frac{2^j}{L}} \epsilon_{jl}^v. \quad (15)$$

Since $\int \phi_{jl}(z) \frac{d}{dz} \phi_{jl'}(z) dz = \frac{2^j}{L} \Omega_{l-l'}^{0,1}$, where $\Omega_{l-l'}^{0,1}$ is the so called connection coefficient of the basic scaling function (e.g. Restrepo & Leaf 1995), Eq.(14) can be rewritten as

$$\epsilon_{jl}^m \simeq -\frac{1+z}{HfD} \sum_{l'=0}^{2^j-1} \frac{2^j}{L} \Omega_{l-l'}^{0,1} \epsilon_{jl'}^v. \quad (16)$$

This is the density-velocity linear Eq.(1) in the DWT representation. It is convenient for estimating $\epsilon_{jl'}^v$ from ϵ_{jl}^m , and *vice-versa*. For D4 wavelet $\Omega_{l-l'}^{0,1}$ is non-zero only for $|l-l'| \leq 2$.

For a Gaussian velocity field, we have $\langle \epsilon_{jl'}^{v_i} \epsilon_{jl''}^{v_i} \rangle = 0$ if $l' \neq l''$ (Pando, Feng & Fang 2001), and therefore, Eq.(16) yields

$$\langle (\epsilon_{jl}^m)^2 \rangle \simeq \frac{(1+z)^2}{(HfD)^2} \sum_{l'=0}^{2^j-1} \left[\frac{2^j}{L} \Omega_{l-l'}^{0,1} \right]^2 \langle (\epsilon_{jl'}^v)^2 \rangle. \quad (17)$$

Moreover, for a uniform and isotropic random field, $\langle (\epsilon_{jl}^m)^2 \rangle$ and $\langle (\epsilon_{jl}^v)^2 \rangle$ are independent of position index l . Eq.(17) gives

$$\langle (\epsilon_{jl}^m)^2 \rangle \simeq \left[\frac{2^j(1+z)}{LHfD} \right]^2 W \langle (\epsilon_{jl}^v)^2 \rangle, \quad (18)$$

where $W = \sum_{|l-l'| \leq 2} (\Omega_{l-l'}^{0,1})^2$.

3.2. Results of *rms* bulk velocity

The ensemble of N Ly α forests can be seen as a sampling of the sky with pencil beams. Because the operation $(1/L_x L_y) \int_{L_x} \int_{L_y} \dots dx dy$ actually is an average over the celestial sphere, it can be statistically approximated by an ensemble average over the sky sampling. That is, the 1-D density perturbation $\delta(r)$ can statistically be estimated by

$$\delta(r) = \frac{1}{L_x L_y} \int_{L_x} \int_{L_y} \delta(x, y, r) dx dy \simeq \frac{1}{N} \sum_{i=1}^N \delta(x_i, y_i, r). \quad (19)$$

Thus, using Eqs.(7), (8), (9) and (12), we have

$$\epsilon_{jl}^m = \int \delta(z) \phi_{jl}(z) dz = \frac{1}{N} \sum_{i=1}^N \int \delta(x_i, y_i, z) \phi_{jl}(z) dz = -\frac{1}{aA(z)} \epsilon_{jl}^F. \quad (20)$$

Substituting Eqs.(20) and (15) into Eq.(18), we finally have the estimator for the *rms* bulk velocity on scale j , $\sigma_j^{v_r} = \langle v_j^r \rangle^{1/2}$, of the underlying mass field of Ly α forests

$$\sigma_j^{v_r} \simeq \frac{Rf(z)}{aA(z)W^{1/2}(1+z)} [2^{J-j} \langle (\epsilon_{jl}^F)^2 \rangle]^{1/2}, \quad (21)$$

where $R = cL/2^J$ is the pixel size in km s^{-1} , and the physical length scale corresponding to j is $cL[2^j H_0 E(z)]^{-1}$. The superscript v_r is to remind that it is a projection along the r -direction. The *rms* bulk velocity on a given scale is then determined from the flux fluctuations δF on the same scale.

Using the estimator Eq.(21), we calculate the *rms* bulk velocities for the three redshift regions $z \pm 0.25$ with $z = 2.25, 2.75$, and 3.25 . The results are presented in Table 1. The scales in Table 1 have the same meaning as those in Fig. 1. In this calculation a is taken to be 1.6, and $R = 293 \text{ km s}^{-1}$. The factor $A(z)$ is calculated from the mean transmission $\langle F(z) \rangle$ in each redshift range via $A(z) = -\ln \langle F(z) \rangle$.

It should be pointed out that the average over N pencil beams in eq.(19) will cause a Poisson error, which then contributes to the variance of $\delta(r)$. This problem is the same as the Poisson correction in calculating the power spectrum of galaxies (Peebles 1980, Fang & Feng 2000). In Table 1 this correction has already been applied.

The errors in Table 1 are calculated from different realizations of phase-randomized spectra which preserves the Gaussianity on large scales (Jamkhedkar, Zhan, & Fang 2000; Zhan, Jamkhedkar, & Fang 2001). It is essentially similar to the bootstrap error estimation (Mo, Jing, & Börner 1992). Besides this error, there are also systematic errors caused by the uncertainties of the factor $aA(z)$ in Eq.(7). For a given redshift range, the uncertainty of the mean transmission $A(z)$ is less than 10%, and the uncertainty of a is about $(1.9-1.5)/1.6 = 25\%$. Therefore, the total systematic error would be about 30%.

Continuum-fitting may cause error if the continua F_c of the 60 QSOs fluctuate significantly on the same scale considered, say $92 \text{ h}^{-1} \text{ Mpc}$. However, the PDFs of ϵ_{jl}^F on large scales are perfectly Gaussian. Therefore, the SFC ϵ_{jl}^F may be significantly contaminated by the continuum fluctuations *only if* the PDF of the continuum fluctuations is also Gaussian. This seems quite unlikely, as the emission from each QSO is highly non-thermal.

All the 1-D *rms* bulk velocities listed in Table 1 are consistent with the assumption in §2, i.e. the peculiar velocity v_r is much smaller than the spatial size considered, i.e. $H_0 r \geq 2300 \text{ km s}^{-1}$. Moreover, the error from the resolution R of the samples is also small,

Table 1: 1-D *rms* bulk velocities $\sigma_j^{v_r}$ (km s^{-1})

Scales (h^{-1}Mpc)	92	46	23
$z = 2.25$	130 ± 50	190 ± 55	230 ± 50
$z = 2.75$	62 ± 40	86 ± 30	94 ± 20
$z = 3.25$	110 ± 45	170 ± 50	190 ± 40

as R is also much less than the spatial size considered. In other words, the position and density uncertainties caused by v_r in Eq.(2) and R are negligible in comparison with the scales listed in Table 1. We should point out that the result of Table 1 is not sensitive to the choice of wavelets. Our analysis relies only on the orthogonality, completeness, and locality of the scaling function. Therefore, all wavelets with compactly supported basis will produce similar results.

As expected, Table 1 shows that σ_v decreases with scales from 23 to 92 $h^{-1}\text{Mpc}$, and it also decreases with redshift from 2.25 to 3.25. However, there is a dip of the bulk velocities on all scales at around $z = 2.75$. This should be verified with other sets of Ly α QSO transmission fluxes.

4. Discussions and conclusions

To properly compare the estimated $\sigma_j^{v_r}$ with other observed or theoretical results, we should emphasize that $\sigma_j^{v_r}$ and v_j are defined by the DWT decomposition of velocity field (Eq.[15]), not by the velocities of particles or galaxies. It has been pointed out recently that the velocity defined by the particle-counting or galaxy-counting method may have different statistical properties from that defined by velocity field decomposition (Yang et al. 2001.) Therefore, we should compare our results with those that are also based on field decomposition if available.

From Eqs.(12) and (15), we have

$$v_j = \frac{\int_{L_x} \int_{L_y} \int v_r(x, y, z) \phi_{jl}(z) dx dy dz}{L_x L_y \int \phi_{jl}(z) dz}. \quad (22)$$

In terms of the DWT analysis, the average $(1/L_x) \int_{L_x} \dots dx$ can be replaced by scaling function projection window $\int \dots \phi_{j_x, l}(x) dx / \int \phi_{j_x, l}(x) dx$, where j_x corresponds to scale L_x . Thus, Eq.(22) can be rewritten as

$$v_j = \frac{\int v_r(x, y, z) \phi_{j_x, l_x}(x) \phi_{j_y, l_y}(y) \phi_{jl}(z) dx dy dz}{\int \phi_{j_x, l_x}(x) \phi_{j_y, l_y}(y) \phi_{jl}(z) dx dy dz} = v_{j_x, j_y, j}. \quad (23)$$

Since the scales L_x and L_y are much larger than the radial scale $L/2^j$ considered, we have $j_x, j_y \ll j$. Therefore, $\sigma_j^{v_r}$ actually is the 1-D *rms* bulk velocity of the 3-D mode (j_x, j_y, j) with $j_x, j_y \ll j$, i.e. $\sigma_j^{v_r} = \langle v_{j_x, j_y, j}^2 \rangle^{1/2} = \sigma_{j_x, j_y, j}^{v_r}$. For a homogeneous and isotropic random mass field with a relatively flat power spectrum around 100-150 Mpc, we have $\sigma_{j, j, j}^{v_r} \simeq \sqrt{3} \sigma_{j_x, j_y, j}^{v_r}$ if $j_x, j_y \ll j$, or equivalently, L_x and L_y are much larger than the physical scales of j (Yang et al 2001).

Since the results listed in Table 1 are derived for high redshifts, there is no directly measured result available for comparison. The bulk velocity in a sphere of radius $50 \text{ h}^{-1}\text{Mpc}$ around the Local Group is found to be $370 \pm 110 \text{ km s}^{-1}$ (Dekel et al 1998). The scale of the sphere is comparable to the linear scale $92 \text{ h}^{-1}\text{Mpc}$ in Table 1. If this result can be considered as the bulk velocity of a box $100^3 \text{ h}^{-3}\text{Mpc}^3$, the corresponding 1-D bulk velocity v_j on scale $100 \text{ h}^{-1}\text{Mpc}$ (with $L_x, L_y \gg 100\text{h}^{-1}\text{Mpc}$) is about $370/\sqrt{3}/\sqrt{3} = 123 \text{ km s}^{-1}$ (the first $\sqrt{3}$ is due to the transform from 3-D to 1-D of the velocity, and the second $\sqrt{3}$ is due to the transform from mode (j, j, j) to $(0, 0, j)$). Considering linear redshift evolution, this 1-D bulk velocity yields 99, 92 and 88 km s^{-1} at redshift $z = 2.25, 2.75$, and 3.25 , respectively. These results are consistent with that shown in Table 1. Nevertheless we should remember that the bulk velocity 370 km s^{-1} is from one realization, not *rms* value, and it may have the uncertainties of galaxy-counting as well as galaxy bias.

The 1-D *rms* bulk velocity in the DWT modes (j, j, j) at redshift $z = 0$ has been calculated from N body simulations. The results on $92 \text{ h}^{-1}\text{Mpc}$ are $60 \pm 10 \text{ km s}^{-1}$, $70 \pm 20 \text{ km s}^{-1}$, and $80 \pm 20 \text{ km s}^{-1}$ for the SCDM, LCDM and τ CDM models respectively (Yang et al 2001). All models give lower *rms* bulk velocity than that shown in Table 1. One cannot, however, conclude that the N body simulated result is inconsistent with that shown in Table 1. This is because the *rms* bulk velocity is sensitive to the perturbation on large scales, while the simulation box in Yang et al (2001) is $256^3 \text{ h}^{-3}\text{Mpc}^3$. It has been pointed out (Tormen & Bertschinger 1996) that the linear 3-D *rms* bulk velocity of a cube of side 100 Mpc is well over 500 km s^{-1} for an SCDM model with $\sigma_8 = 1$. Correspondingly, for an LCDM model with $\sigma_8 = 0.7$ the 1-D *rms* bulk velocities of DWT mode $(L_x, L_y, 92 \text{ h}^{-1}\text{Mpc})$, i.e. $\sigma_{0,0,j}^{v_r}$, are 110 km s^{-1} , 105 km s^{-1} , and 100 km s^{-1} at $z = 2.25, 2.75$, and 3.25 respectively. Therefore, the results shown in Table 1 basically are consistent with the linear evolution theory within 1σ confidence level.

We should also emphasize that the average over a QSO ensemble, i.e. average over the celestial sphere, is important. The errors in Table 1 also comes from the fact that the number of Ly α forests in a given redshift bin is still small (large Poisson correction caused by eq.[19]). Nevertheless, one can already conclude that a set of Ly α forests can provide a valuable estimate of the *rms* bulk velocity of the underlying mass field on scales from a few tens to $\lesssim 100 \text{ h}^{-1}\text{Mpc}$. With a large set of Ly α forests, one may map the bulk velocity on large scales in a wide range of redshift, and then, set a robust constraint on the power spectrum on large scales.

The authors would like to thank David Burstein for helpful suggestions.

REFERENCES

Bechtold, J. 1994, ApJS, 91, 1

Bi, H.G. 1993, ApJ, 405, 479

Bi, H.G., & Davidsen, A. F. 1997, ApJ, 479, 523.

Bi, H.G., Ge, J., & Fang, L.Z. 1995, ApJ, 452, 90

Brachini, E., Teodoro, L., Frenk, C.S., Schmoldt, I., Efstatthiou, G., White, S.D.M., Saunders, W., Sutherland, W., Rowan-Robinson, M., Keeble, O., Tadros, H., Maddox, S., & Oliver, S. 1999, MNRAS, 308, 1

Croft, R.A.C., Weinberg, D.H., Katz, N., & Hernquist, L. 1998, ApJ, 495, 44

Croft, R.A.C., Weinberg, D.H., Pettini, M., Hernquist, L., & Katz, N. 1999, ApJ, 520, 1

Daubechies I. 1992, *Ten Lectures on Wavelets* (Philadelphia: SIAM)

Dekel, A. 1998, Formation of Structure in the Universe, eds. Dekel, A., & Ostriker, J. (New York: Cambridge Univ. Press)

Dekel, A., Eldar, A., Kolatt, T., Yahil, A., Willick, J.A., Faber, S.M., Courteau, S., & Burstein, D. 1999, ApJ, 522, 1

Dobrzański, A. & Bechtold, J. 1996, ApJ, 457, 102

Fang, L.Z., Bi, H.G., Xiang, S.P., & Börner, G. 1993, ApJ, 413, 477

Fang, L.Z. & Feng, L.L. 2000, ApJ, 539, 5

Fang, L.Z. & Thews, R. 1998, *Wavelet in Physics* (Singapore: World Scientific)

Farge, M., Kevlahan, N., Perrier, V., & Goirand, É. 1996, Proceedings of the IEEE, 84, 639

Feng, L.L. & Fang, L.Z. 2000, ApJ, 535, 519

Feng, L.L. Pando, J., & Fang, L.Z. 2001, ApJ, 555, 74

Hui, L. 1999, ApJ, 516, 519

Hui L. & Gnedin, N.Y. 1997, MNRAS, 292, 27

Jamkhedkar, P., Bi, H.G., & Fang, L.Z. 2001, ApJ, in press, astro-ph/0107185

Jamkhedkar, P., Zhan, H., & Fang, L.Z. 2000, ApJ, 543, L1

Lahav, O., Rees, M. J., Lilje, P. B., & Primack, J. R. 1991, MNRAS, 251, 128

McDonald, P. & Miralda-Escudé, J. 1999, ApJ, 518, 24

McDonald, P., Miralda-Escudé, J., Rauch, M., Sargent, W.L.W., Barlow, T. A., Cen, R., & Ostriker, J. P. 2000, ApJ, 543, 1

Mo, H. J., Jing, Y. P., & Börner, G. 1992, ApJ, 392, 452
Nusser, A. & Haehnelt, M. 1999, MNRAS, 303, 179
Pando, J., Feng, L.L., & Fang, L.Z. 2001, ApJ554, 841.
Peebles, P. J. E., 1980, *Large Scale Structure of the Universe* (Princeton: Princeton University Press)
Rauch, M. 1998, ARA&A, 36, 267
Restrepo, J.M. & Leaf, G.K. 1995, J. of Computational Phys. 122, 118
Scott, J., Bechtold, J., & Dobrzański, A. 2000, ApJS, 130, 37
Scott, J., Bechtold, J., Dobrzański, A., & Kulkarni, V. 2000, ApJS, 130, 67
Tormen, G. & Bertschinger, E. 1996, ApJ, 472, 14
Yang, X.H., Feng, L.L., Chu, Y.Q., & Fang, L.Z. 2001, ApJ, in press, astro-ph/0107083
Zhan, H., Jamkhedkar, P., & Fang, L.Z. 2001, ApJ, 555, 58

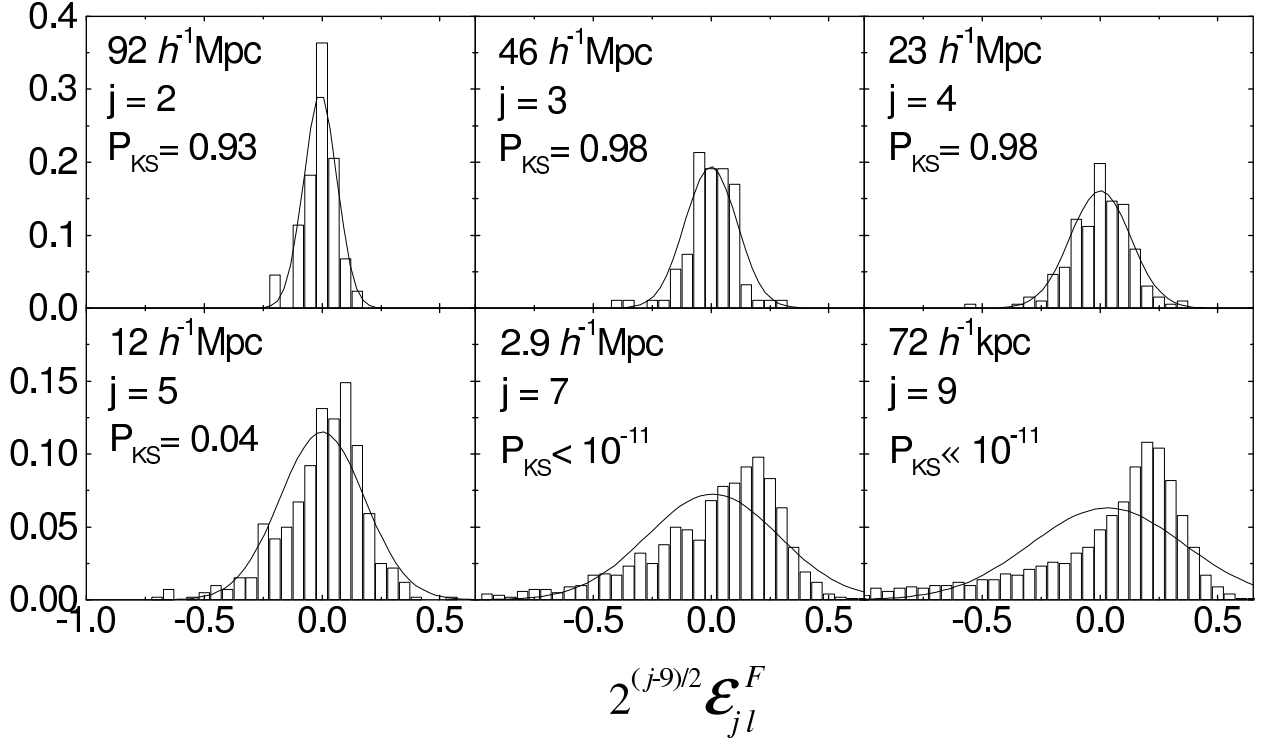


Fig. 1.— Probability distribution functions of ϵ_{jl}^F s of the data set consisting of all QSO spectrum segments within the redshift range from 2.5 to 3.0. An LCDM ($\Omega = 0.3$ and $\Lambda = 0.7$) universe is assumed to calculate the comoving length scales. P_{KS} is the K-S probability of the PDF being Gaussian.